Environmental Acoustics and Intensity Vector Acoustics with Emphasis on Shallow Water Effects and the Sea Surface

Peter H. Dahl
Applied Physics Laboratory
University of Washington
Seattle, Washington 98105
phone: (206) 543-2667 fax: (206) 543-6785 email:dahl@apl.washington.edu

LONG-TERM GOALS

To understand and predict key properties of the signal intensity vector field in forward propagation with emphasis on mid-frequency, shallow water propagation. Because of enabling technologies involving MEMS and bio-inspired transduction, tomorrow's navy will depend on and utilize acoustic vector field properties (velocity, acceleration, intensity) much more than today's. Advancement in Navy relevant capabilities will be in part realized through a better understanding of the environmental and acquisition geometry dependence (source depth, range, etc.) of the vector field in a shallow water environment.

OBJECTIVES

The primary technical objective this year was analyze was to (1) procure a VHS-100 vector sensor from China and test it in a controlled setting, (2) complete analysis on a new approach to obtain geoacoustic properties from vector quantities using data from Shallow Water 06 (SW06) experiment off the coast of New Jersey (2006) , and (3) complete a study on the effect of directional waves (from SW06.)

APPROACH

Key individuals are doctoral graduate student David Dall'Osto (APL-UW and UW Mechanical Engineering supported by OA Graduate Traineeship Award) who worked on PE simulations of the vector field, on SW06 data analysis, and conducted measurements with the VHS-100, and William Plant (APL-UW) who worked on simulation of rough surfaces at both large and small scale.

Objectives (1) and (2) are closely linked and are discussed in detail here. (These objectives are closely linked to Dall'Osto's Ph.D. dissertation, the first part of which is published in [1].) The main focus of the vector acoustic research has been measuring and understanding properties of vector intensity under various propagation conditions. The physical interpretation of the active and reactive intensity relates to acoustic particle motion, which we can measure with an accelerometer based vector sensor. In a purely active field (e.g. the free-field a few wavelengths from a point source) the particle motion follows a back and forth motion along a line oriented outward from the source. The field of this same source near a reflecting boundary will no longer be purely active. The reflection from the wall, which can be viewed as the field due to an image source on the other side of the wall with relative phase of the direct and reflected fields influencing the motion of the fluid particle. If the two wavefronts are in phase, acoustic particle motion falls along a line with an orientation related to the relative magnitude of the direct and reflected field. When the two wavefronts are

Report Documentation Page

Form Approved
OMB No. 0704-0188

Public reporting burden for the collection of information is estimated to average 1 hour per response, including the time for reviewing instructions, searching existing data sources, gathering and maintaining the data needed, and completing and reviewing the collection of information. Send comments regarding this burden estimate or any other aspect of this collection of information, including suggestions for reducing this burden, to Washington Headquarters Services, Directorate for Information Operations and Reports, 1215 Jefferson Davis Highway, Suite 1204, Arlington VA 22202-4302. Respondents should be aware that notwithstanding any other provision of law, no person shall be subject to a penalty for failing to comply with a collection of information if it does not display a currently valid OMB control number.

1. REPORT DATE **2012**	2. REPORT TYPE **N/A**	3. DATES COVERED **-**

4. TITLE AND SUBTITLE **Environmental Acoustics and Intensity Vector Acoustics with Emphasis on Shallow Water Effects and the Sea Surface**	5a. CONTRACT NUMBER
	5b. GRANT NUMBER
	5c. PROGRAM ELEMENT NUMBER
6. AUTHOR(S)	5d. PROJECT NUMBER
	5e. TASK NUMBER
	5f. WORK UNIT NUMBER
7. PERFORMING ORGANIZATION NAME(S) AND ADDRESS(ES) **Applied Physics Laboratory University of Washington Seattle, Washington 98105**	8. PERFORMING ORGANIZATION REPORT NUMBER
9. SPONSORING/MONITORING AGENCY NAME(S) AND ADDRESS(ES)	10. SPONSOR/MONITOR'S ACRONYM(S)
	11. SPONSOR/MONITOR'S REPORT NUMBER(S)

12. DISTRIBUTION/AVAILABILITY STATEMENT
Approved for public release, distribution unlimited

13. SUPPLEMENTARY NOTES
The original document contains color images.

14. ABSTRACT

15. SUBJECT TERMS

16. SECURITY CLASSIFICATION OF:			17. LIMITATION OF ABSTRACT **SAR**	18. NUMBER OF PAGES **8**	19a. NAME OF RESPONSIBLE PERSON
a. REPORT **unclassified**	b. ABSTRACT **unclassified**	c. THIS PAGE **unclassified**			

**Standard Form 298 (Rev. 8-98)**
Prescribed by ANSI Std Z39-18

out of phase, the motion follows a curved path which will be purely circular when the two wavefronts are of equal magnitude and 90 degrees out of phase.

This motion can be succinctly described by degree of circularity, which itself is a vector and defined as follows [2] ,

$$\bar{\Theta} = 2\frac{\mathrm{Im}\{\bar{\mathbf{v}} \times \bar{\mathbf{v}}^*\}}{|\bar{\mathbf{v}}|^2} = 2\frac{\bar{\mathbf{Q}} \times \bar{\mathbf{I}}}{|p|^2 |\bar{\mathbf{v}}|^2} \qquad\qquad [1]$$

where $\bar{\Theta}$ is dependent on the relative orientation of the active intensity, $\bar{\mathbf{I}}$, and reactive intensity, $\bar{\mathbf{Q}}$, vectors and is non-dimensionalized by normalizing by the magnitude of the pressure and particle velocity fields. Note that circularity as described in Eq.(1) relates closely to the pressure-velocity index discussed in [1] in the context of measurements taken in Korean waters. The values of $\bar{\Theta}$ fall between +/-1 where 0 indicates a particle motion path falling entirely on a straight line and +/-1 indicates purely circular motion in a counter-clockwise or clockwise direction, respectively. In general, circular motion occurs in regions of destructive interference, while straight line motion occurs in regions of constructive interference.

Figure 1 illustrates the various types of motion we can measure with a tri-axial accelerometer based sensor. Note that particle velocity will be confined effectively to the u and v components, the resulting in-plane circularity becomes a scalar ranging between +/- 1.
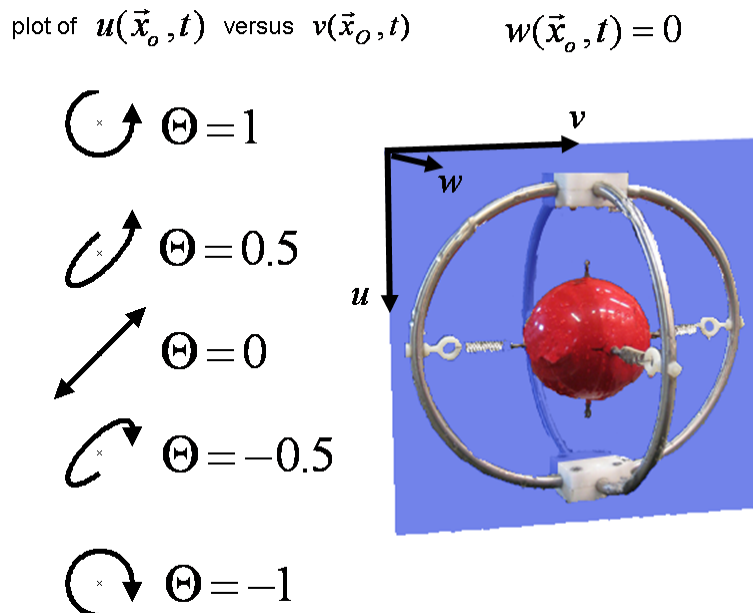

Figure 1. Illustration of various types of particle motion with corresponding value Θ. The red sphere on the left is a VHS-100 vector sensor suspended within a cage as necessary for its operation as a neutrally buoyant device.

WORK COMPLETED

Measurements of circularity using the VHS-100 sensor were made in experiment conducted at the Applied Physics Laboratory's acoustic test facility (ATF) by vertically profiling a simple interference field of an underwater, near-surface source. The resulting measurements of Θ in the source/receiver plane agree with the

theoretical values predicted by the characteristic Lloyd mirror pattern. Furthermore, these measurements confirmed the ability to approximate Θ solely from vertical measurements, by estimating the horizontal component of active intensity from the total pressure magnitude and the vertical component of active intensity, and asserting that the horizontal reactive intensity is zero. The results of this experiment, including a comparison of Θ and its approximation from the vertical intensity, are presented in Fig. 2. The close agreement between the true Θ and its approximate value give sufficient justification to apply this estimation concept for circularity in particle motion to experimental vertical intensity data from the SW06 as discussed next.
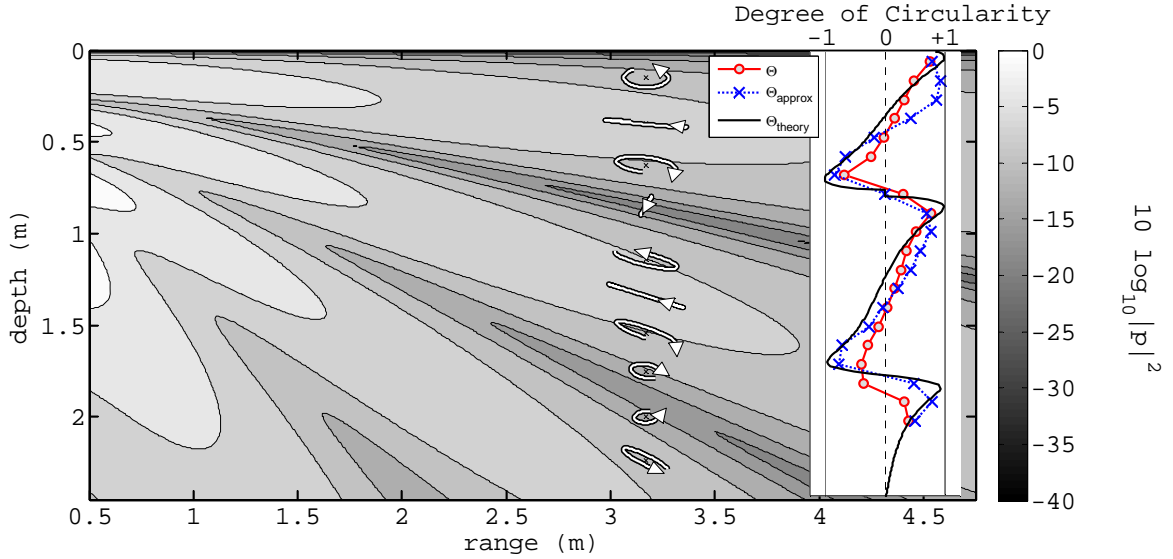
Figure 2. Contours of pressure magnitude of the theoretical Lloyd Mirror interference field at 3kHz as a function of range and depth based on a source at depth 1 m. Superposed on these contours are measurement results from the VHS-100 vector sensor positioned at range 3.17 m and depths from just below the surface (near 0 m) to 2 m depth. The first result shows the exaggerated displacement vector (obtained by twice integrating the acceleration channels from the VHS-100) as indicated by the arrows at the measurement depths. The second result shows estimates of circularity (red symbols) compared with theoretical estimates (black symbols), and approximate estimates of Θ derived from the vertical intensity (blue symbols).

A very important and exploitable feature of the Θ is its sensitivity to interference; for example how it relates directly the angles of interfering wavefronts and therefore reflection and refraction processes in a waveguide. We demonstrate this next using data originating from Shallow Water 06 (SW06) off the coast of New Jersey, for which a characteristic pattern emerges in the range dependence of Θ. The experimental configuration (Fig. 3) consists of a towed source emitting 1-kHz tone burst from a source approximately 4 m above the sea-floor. The relative propagation angles of the interfering direct, bottom and sub-bottom arrivals correspond to a change in circularity (from clockwise to counter-clockwise) in range. Importantly, this occurs at a characteristic wavelength, λ_θ, which we later exploit for purposes of geoacoustic inversion. The propagation angles, thus λ_θ, can be readily computed using ray theory which are sensitive to the environmental parameters of the top-layer of sediment, specifically the thickness (H_s) and sound speed (c_s).
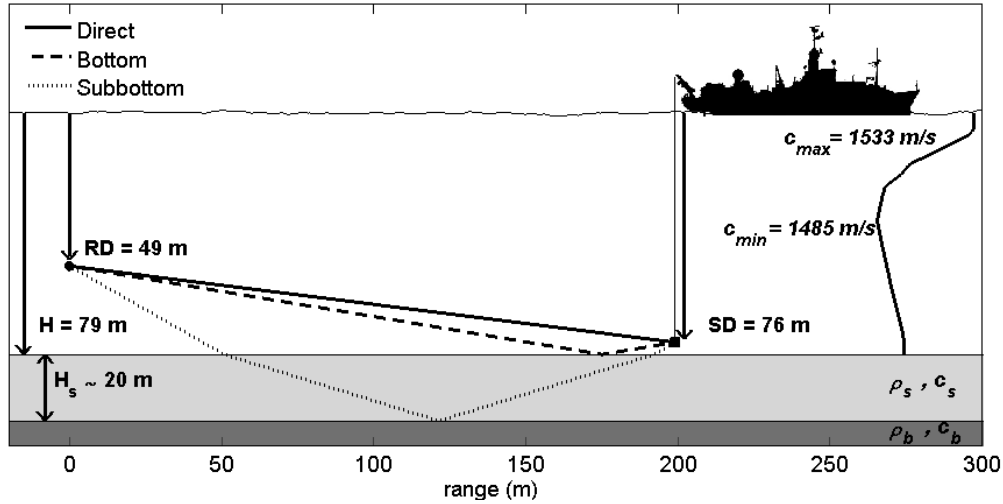
*Figure 3. Experimental configuration for the SW06 bottom-layer study.*

A simulation capability was developed to accurately compute vector acoustic fields, and vector intensity fields in an underwater waveguide through modification of the RAM parabolic wave equation (PE) code [3]. The vector products of the PE are used to construct Θ as a function of time, range and depth. Using ray theory to predict the arrival times of the main arrival, estimates of Θ during the interference can be constructed as a function of range and depth. Both approaches produce very similar estimates of Θ for a parameterized bottom using a nominal depth H_s of 20 m and a sediment sound speed of 1600 m/s. (These estimates are discussed in the context of inversion error in Fig. 4.)

Circularity as a function of range and depth for a particular bottom model is shown in Fig. 4. The black and white image is a reduced, or simplified image, giving just the sign of circularity, i.e., +/-1, and it is computed with PE. The horizontal streaks near the surface are a manifestation of interference with the sea surface, and the critical area of interest is that shown within the red circle. The plot immediately below the black and white image is a cut of circularity at depth 49 m. Between ranges 200 and 250 m, there is a significant interference effect as shown by the change in sign in circularity. The interference wavelength λ_θ, is an essential observation which we subsequently invert for sea bed parameters. We note here that the region generally encompassed by the red circle can readily be studied using the method of images, in this case where the image reflection is from the seabed, and a spherical wave reflection coefficient analysis is used. Although inclusion of spherical wave effects complicates matters, the total modeling effort with this approach is orders of magnitude faster than one involving vector products from broad band PE.

4
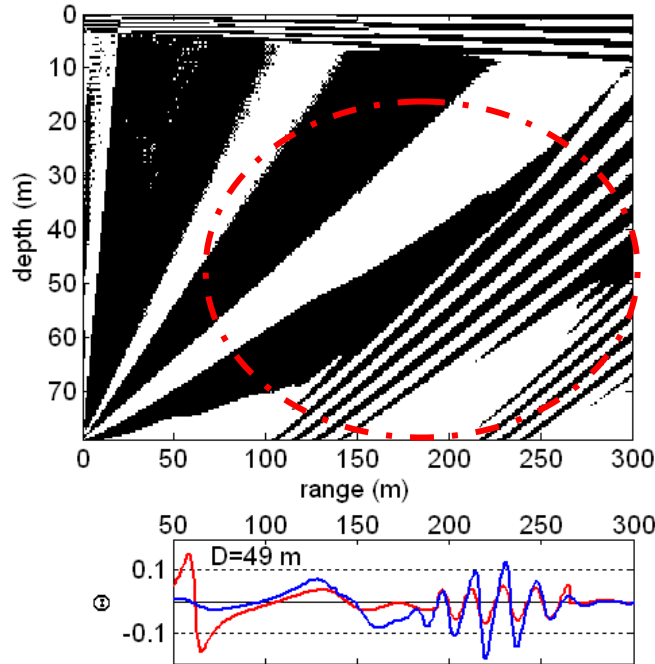
Figure 4 – (Top) An image of the PE calculated sign of Θ constructed from a broadband synthesized signal, where black is negative and white is positive. The red circle indicates a region where the image method can be used to estimate Θ. (Bottom) The value of Θ at depth 49 m (blue) as a function of range is shown along with the image method result using the spherical wave reflection coefficient (red).

The experimental data at the depth 49 m can be inverted by a least squares fit. The sensitivity of this parameter to changes with the value of the estimate, can be determined from the Fisher information matrix (FIM) constructed from the image method due to its computational simplicity. There is some uncertainty into estimating λ_θ, over three experimental measurements the estimate of λ_θ varied by ~1 m. This uncertainty was confirmed by an analysis of PE data contaminated with Gaussian white noise of various SNR, the value at the experimental SNR of 30 dB puts this uncertainty equal to +/- 1.12 m. The best parameter estimate of the data and the uncertainty, with respect to the estimated variance of λ_θ ($\sigma_\lambda^2 = 1.25$ m^2), are c_s = 1615 m/s +/- 8 m/s and H_s = 16 m +/- 3.5 m. These parameter estimate uncertainties are summarized in the plot of the error ellipses (Fig. 5) determined by an analysis of the Cramer-Rao Lower Bound (CRLB) and eigenvectors of FIM. The values within the oval show the uncertainty of each parameter for an estimate located in the oval center. The eigenvectors of the FIM, which describe its off-diagonal terms, show how errors in parameter estimates are related, i.e., were the off-diagonal terms to be zero the errors are not correlated. This is important to consider when estimating parameters using an adaptive algorithm, and a change in direction of the vectors may require a change in the order in which to estimate the parameters[4]. These results are discussed in the paper by Dall'Osto and Dahl (July 2012) presented at the European Conference on Underwater Acoustics, which is also the subject of a manuscript submitted to the *J. Acoust. Soc. Am.* The more recent submission provide further details on the estimation technique and the CRLB analysis.
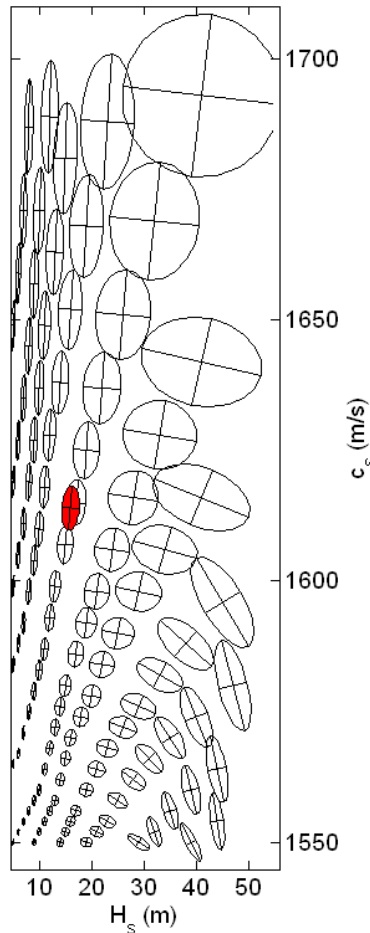
Figure 5 – Summary of the uncertainties of Θ where the uncertainty of the parameter pair H_s,c_s centered at the crosses are given by the error ellipse. The eigenvectors of the FIM set the major and minor axis of an error ellipse, and where they are not perpendicular (on the scaling of this plot) indicates errors are correlated. The uncertaintiy associated with the best estimate is given by the red error-ellipse.

We conclude the WORK COMPLETED section with brief mention of our work involving sea surface scattering. Figure 6 shows estimates of the vertical spatial coherence of sound forward scattering from the sea surface, for which the center frequency of the transmit pulse, sufficiently short to isolated just the surface bounce path, is 6 kHz. The key point here is that measurements made at two orthogonal directions, identified by the red and blue curves, are statistically different. This difference is due to properties of the sea surface directional wave spectrum, and, importantly, the difference is successfully modeled using broad band PE methods, in conjunction with synthetic sea surfaces generated from the corresponding measured directional wave spectrum. Details are discussed in the paper by Dahl, *et al* (May 2012).
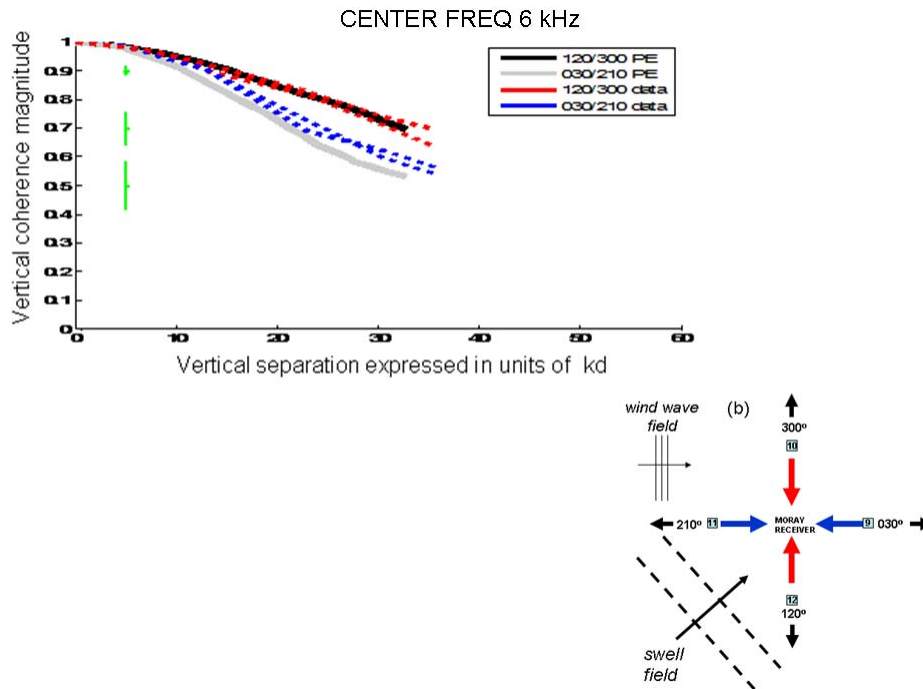
Figure 6 (Top) Vertical coherence magnitude for surface bounce path at range 200 m, center frequency 6 kHz, as a function of normalized receive separation (kd) for a 1.5 m aperture. Measurements (data) and (PE) modeling corresponding to two orthogonal source-receiver directions are indicated identified in the legend. Error bars correspond to 3 particular estimates of coherence magnitude based on 40 degrees of freedom which corresponds to the measurements. (Lower Right) Source-receiver directions with respect to the sea surface directional wave field with color code corresponding to the legend in the upper plot.

IMPACT/APPLICATIONS

The knowledge base gained from these objectives applies directly to vector sensing technologies, prediction of bottom and sea-surface reverberation, and model development for shallow water acoustics that focuses on both scalar and vector quantities.

Our work on the effects of the directional wave spectrum has a direct impact on reverberation in shallow water, e.g., lower coherence indicates larger vertical angular width, which in turn influence both propagation loss (through mode stripping) and reverberation from the sea bed. Laboratory measurements using the VHS-100 vector sensor such as those shown in Fig. 2 are also geared towards use of this new sensor in the upcoming TREX13 experiment in the Gulf of Mexico in spring 2013; measurements like those discussed in Fig. 6 will be a essential part of the upcoming TREX 13 experiment.

RELATED PROJECTS

The PI is also advising PhD student Mr. Jeffrey Daniels, from the Acoustics Research Detachment (Bayview ID) Carderock Division, who has received an ILIR grant from ONR to study new vector sensing technologies at the University of Washington.

REFERENCES

[1] D. R. Dall'Osto, P. H. Dahl and J. W. Choi "Properties of the acoustic intensity vector field in a shallow water waveguide," J. Acoust. Soc. Am. Volume 131(3), p. 2023-2035 (2012).

[2] Gerald L. D'spain, "Polarization of acoustic particle motion in the ocean and its relation to vector acoustic intensity," Proceedings of the 2nd International Workshop on Acoust. Eng. and Tech. Harbin, China (1999).

[3] M. D. Collins, "A split-step Padé solution for the parabolic equation method," J. Acoust. Soc. Am., 93, 1736-1742, 1993.

[4] H. Schmidt and A.B. Baggeroer, "Physics-imposed resolution and robustness issues in seismo-acoustic parameter inversion," Modern Approaches in Geophysics Vol. 12, Full Field Inversion Methods in Ocean and Seismo-Acoustics, 85-90. (1995).

PUBLICATIONS

D. R. Dall'Osto and P. H. Dahl, Waveguide properties of active intensity vorcity, Proceedings of the 11th European Conference on Underwater Acoustics (9 pages), Edinburgh, July 2012.

Dahl P.H, D.R. Dall'Osto, and W. J. Plant, "The sea surface directional wave spectrum and forward scattering from the sea surface," Invited paper published in the *Proceedings of Acoustics 2012,* Hong Kong (6 pages), May 2012.

G. Kapodistrias and P H. Dahl, "Scattering measurements from a dissolving bubble, " *J. Acoust. Soc. Am.* 131, 4243-4251, June 2012